© 2016. Published by The Company of Biologists Ltd | Journal of Experimental Biology (2016) 219, 508-515 doi:10.1242/jeb.127662

RESEARCH ARTICLE

FRET analysis using sperm-activating peptides tagged with fluorescent proteins reveals that ligand-binding sites exist as clusters

César Arcos-Hernández, Francisco Romero, Yoloxochitl Sánchez-Guevara, Carmen Beltrán and Takuya Nishigaki*

ABSTRACT

Long-range cellular communication between the sperm and egg is critical for external fertilization. Sperm-activating peptides (SAPs) are diffusible components of the outer layer of eggs in echinoderms, and function as chemoattractants for spermatozoa. The decapeptide named speract is the best-characterized sea urchin SAP. Biochemical and physiological actions of speract have been studied with purified or chemically synthesized peptides. In this work, we prepared recombinant speract fused to a fluorescent protein (FP; FP-speract) using three color variants: a cyan (eCFP), a yellow (mVenus) and a large Stokes shift yellow (mAmetrine) FP. Although these fluorescence tags are 20 times larger than speract, competitive binding experiments using mAmetrine-speract revealed that this FP-speract has binding affinity to the receptor that is comparable (7.6-fold less) to that of non-labeled speract. Indeed, 10 nmol l^{-1} eCFP-speract induces physiological sperm responses such as membrane potential changes and increases in intracellular pH and Ca^{2+} concentrations similar to those triggered by 10 nmol l^{-1} speract. Furthermore, FP-speract maintains its fluorescence upon binding to its receptor. Using this property, we performed fluorescence resonance energy transfer (FRET) measurements with eCFP-speract and mVenus-speract as probes and obtained a positive FRET signal upon binding to the receptor, which suggests that the speract receptor exists as an oligomer, at least as a dimer, or alternatively that a single speract receptor protein possesses multiple binding sites. This property could partially account for the positive and/or negative cooperative binding of speract to the receptor.

KEY WORDS: Recombinant peptide ligand, Fluorescence resonance energy transfer, Receptor, Speract

INTRODUCTION

In most marine animals, spermatozoa and eggs are released into the ocean, where the distance between gametes increases upon dilution, which implies a potential problem in achieving successful fertilization for any species. To overcome this problem, marine animals commonly produce a large number of gametes, although there is a trade-off between their number and size. In the case of echinoderms, female gametes employ two additional strategies to improve sperm–egg interactions. One is an increase in physical size by swelling an extracellular matrix, called the egg jelly, through the absorption of seawater (Podolsky, 2002). The other is the release of specific chemoattractants for spermatozoa, sperm-activating peptides (SAPs) (Suzuki, 1995). SAPs initiate their physiological action on spermatozoa through an increase in cyclic guanosine monophosphate (cGMP) levels (Garbers, 1989; Kaupp et al., 2003), which induces membrane potential (V_m) changes (Galindo et al., 2000; Strünker et al., 2006), leading to increases in intracellular pH (pH_i) and Ca^{2+} concentrations ($[Ca^{2+}]_i$) (Nishigaki et al., 2001; Seifert et al., 2015). Changes in $[Ca^{2+}]_i$ in particular play a fundamental role in the regulation of the shape of flagellar beating (Böhmer et al., 2005; Wood et al., 2005), namely, in the process of sperm chemotaxis (Alvarez et al., 2012; Guerrero et al., 2010).

Since the first SAP (speract) was purified and structurally determined (Suzuki, 1995), almost 100 SAPs have been identified from many species of echinoderms (Nishigaki et al., 1996; Suzuki, 1995). SAPs are classified into five or six groups depending on their structures and cross-activities (Suzuki, 1995). There are many isoforms in the same class of SAPs given the existence of isoforms within and among species. The diversity of SAPs within species is attributed to the biosynthesis of these peptides. The mRNA encoding speract and asterosap (SAP isolated from the starfish *Asterias amurensis*) revealed that SAPs are produced as large precursor proteins containing many SAPs isoforms: 9–12 isoforms of speract separated by a single amino acid (Lys) (Kinoh et al., 1994; Ramarao et al., 1990) and approximately 10 isoforms of asterosap separated by a 12–22 amino acid spacer peptide (Matsumoto et al., 1999; Nakachi et al., 2008). Multiple copies of the same peptide in a single precursor protein were also reported for sarafotoxin in a snake venom (Ducancel et al., 1993), suggesting an efficient strategy for producing a high concentration of similar peptides.

The signal transduction of SAPs has been intensively studied in two species of sea urchin, *Strongylocentrotus purpuratus* (Darszon et al., 2011) and *Arbacia punctulata* (Kaupp et al., 2008), using their corresponding SAPs, speract and resact, respectively. Although the overall signaling cascades are quite similar between these two species, the molecular identities of the ligand receptors are different. Although the resact receptor is a membrane form of guanylyl cyclase (GC) (Singh et al., 1988), speract binds to a 77 kDa Cys-rich protein (Dangott and Garbers, 1984; Dangott et al., 1989) that somehow activates a membrane GC. One fascinating question is how distinct ligand–receptor combinations evolved without altering the overall signaling cascade in echinoderms. It is worth mentioning that speract and its isoforms are produced in accessory cells (somatic cells) of the oocyte (Kinoh et al., 1994), whereas asterosap, which directly binds to GC, is produced in the oocyte itself (Matsumoto et al., 1999).

Speract is the first identified SAP (Gly-Phe-Asp-Leu-Asn-Gly-Gly-Gly-Val-Gly) and its structure–function relationship is well

Departamento de Genética del Desarrollo y Fisiología Molecular, Instituto de Biotecnología, Universidad Nacional Autónoma de México (IBT-UNAM), Av. Universidad 2001, Col. Chamilpa, Cuernavaca, Mor. 62210, Mexico.

*Author for correspondence (takuya@ibt.unam.mx)

Received 1 July 2015; Accepted 20 November 2015

Journal of Experimental Biology

Journal of Experimental Biology (2016) 219, 508-515 doi:10.1242/jeb.127662

List of abbreviations

ASW	artificial seawater
BSA	bovine serum albumin
$[Ca^{2+}]_i$	intracellular Ca^{2+} concentration
cGMP	cyclic guanosine monophosphate
DASW	diluted artificial seawater
eCFP	a variant of enhanced cyan fluorescent protein
FP	fluorescent protein
FP-speract	speract tagged with a fluorescent protein
FRET	fluorescence resonance energy transfer
F-speract	fluorescein-labeled speract
GC	guanylyl cyclase
IPTG	isopropyl-β-D-1-thiogalactopyranoside
LB	Luria broth
pH_i	intracellular pH
SAP	sperm-activating peptide
sNHE	sperm-specific Na^+/H^+ exchanger
V_m	membrane potential

known thanks to the existence of many natural isoforms (Suzuki, 1995) and some synthetic analogues (Garbers et al., 1982; Nomura and Isaka, 1985; Tatsu et al., 2002) of this peptide. Interestingly, the most important residue is the Gly at position six, as its substitution by any amino acid results in at least a 1000-fold decrease in the affinity to its receptor (Tatsu et al., 2002). For biochemical and physiological studies, speract and its analogues (or isoforms) have been obtained by purification of natural peptides or by chemical synthesis. To explore the usefulness of recombinant speract in this study, we prepared three recombinant versions of this peptide fused to fluorescent proteins (FPs) produced in *Escherichia coli* as fluorescent analogues. Although these FP-labeled speracts (FP-speracts) are more than 20 times larger than the intact speract, these ligands are active and have binding affinity comparable to that of the natural ligand. The existence of many color variations of FPs facilitated preparation of FP-speract with different optical properties, which allowed us to perform distinct bioassays using fluorescence spectroscopy to evaluate the ligand activity of FP-speract. Moreover, we determined the proximity of speract binding sites on the sperm plasma membrane using the cyan and yellow variant of FP-speract as a FRET pair, which provided us with new insight into the speract receptor.

MATERIALS AND METHODS

Materials

Sexually mature *Strongylocentrotus purpuratus* (Stimpson 1857) sea urchins were obtained from Pamanes (Ensenada, Baja California, México) and *Lytechinus pictus* (Verrill 1867) from Marinus (Long Beach, CA, USA). Dry sperm were collected after intracoelomic injection of 0.5 mol l^{-1} KCl, and were kept on ice until used. Klenow Fragment, HindIII, XhoI, XbaI, NcoI, T4 ligase, GeneJET Plasmid Miniprep kit, GeneJET Gel Extraction Kit, DNA Ladders and Ni-NTA Superflow agarose were from Thermo Scientific (Waltham, MA, USA). Vent DNA polymerase was from New England Biolabs (Ipswich, MA, USA). Citifluor was from Electron Microscopy Sciences (Hatfield, PA, USA). The fluorescent dyes BCECF-AM, 3,3′-dipropylthiadicarbocyanine iodide [$DiSC_3(5)$] and Fluo-4-AM were obtained from Invitrogen-Molecular Probes (Eugene, OR, USA). cOmplete™ Protease Inhibitor Cocktail Tablets were from Roche (Basel, Schweiz). Luria Broth (LB; containing tryptone, yeast extract and NaCl), kanamycin and the rest of the reagents were from Sigma-Aldrich. Synthetic speract was provided by Dr Tatsu (AIST, Ikeda, Japan) and fluorescein-labeled speract (F-speract) was prepared as described previously (Nishigaki and Darszon, 2000). Artificial seawater (ASW) contained in mmol l^{-1}: 486 NaCl, 27 $MgCl_2$, 29 $MgSO_4$, 10 $CaCl_2$, 10 KCl, 2.5 $NaHCO_3$, 0.1 EDTA, 10 HEPES, pH 8.0 and 1000 mOsm l^{-1}. Low-Ca^{2+} ASW contained 1 mmol l^{-1} Ca^{2+}, pH 7.0. Sperm were swollen as described elsewhere (Babcock et al., 1992; Reynaud et al., 1993) in 10-fold diluted ASW (DASW) supplemented with 20 mmol l^{-1} $MgSO_4$, 120–160 mOsM, pH 6.8. The *E. coli* strains JM109(DE3) and BL21(DE3) were obtained from the National BioResource Project *E. coli* strain, National Institute of Genetics, Mishima, Japan. Plasmids encoding eCFP-pRSETB (Kotera et al., 2010), mVenus-pRSETB (Nagai et al., 2002) and pmAmetrine1.2 (Ding et al., 2011) were provided by Dr T. Nagai (Osaka University), Dr A. Miyawaki (RIKEN) and Dr R. Campbell (University of Alberta, Addgene plasmid no. 42171), respectively.

Construction of plasmids for FP-speract

We used a modified pET28c (Novagen) as expression vector for the recombinant proteins. Using the following two primers, 5′ CCC TCT AGA AAT AAT TTT GTT TAA CTT TAA GA and CCC AAG CTT ATA TCT CCT TCT TAA AGT TAA AC 3′, a double-stranded DNA was synthesized using Klenow Fragment. This double-stranded DNA was double digested with XbaI/HindIII and inserted into a pET28c vector using the same restriction enzymes as cloning sites. Consequently, the modified pET28c, called pET28HindIII, lost approximately 120 bp of pET28c, including NcoI as translation initiation site and the majority of other multi-cloning sites of the original vector.

The three plasmids encoding enhanced cyan fluorescent protein (eCFP), mVenus and mAmetrine (mAmetrine1.2) were separately used as a template and the PCRs were carried out to obtain a single DNA fragment that encodes the entire open reading frame of each FP-speract. Oligonucleotide primers for the PCR are as follows: a forward primer (5′ CCA AGC TTA TGC ATC ATC ATC ACC ACC ACG TGA GCA AGG GCG AGG AGC TGT TC 3′) and a reverse primer (5′ CCC CTC GAG TTA GCC CAC ACC GCC ACC GTT CAG ATC AAA GCC GCC ACC GCC GCT ACC ACC ACC CTT GTA CAG CTC GTC CAT GCC GAG 3′). The forward primer encodes a HindIII site and 6xHis tag followed by the N terminus of these FPs. The reverse primer encodes an XhoI site, a stop codon, speract, seven amino acids as a linker (Gly-Gly-Gly-Ser-Gly-Gly-Gly) and the C terminus of these FPs. All PCRs were performed with two units of Vent DNA Polymerase, 0.3 µmol l^{-1} primers, 100 ng template and 200 µmol l^{-1} of each dNTP in 50 µl using the following thermal cycle: 3 min at 96°C, 35× (30 s at 96°C; 50 s at 58°C; 1 min at 72°C) and 1 min at 72°C. Each PCR produced a single DNA band of approximately 800 bp. The PCR products were purified, double digested with HindIII/XhoI, and inserted into pET28HindIII vector using the same restriction enzymes as cloning sites. The ligated products were used to transform Ca^{2+}-competent JM109 (DE3) cells. Several colonies were inoculated in 3 ml LB medium without isopropyl-β-D-1-thiogalactopyranoside (IPTG) and incubated overnight at 37°C at 200 rpm. After centrifugation of the cell suspension, the pellets of bacteria containing the expected plasmids showed the corresponding colors of each FP (we confirmed the presence of mAmetrine through excitation with 405 nm light as it had a faint yellow color). DNA sequences of the open reading frame of each FP-speract were confirmed by the DNA sequencing facility of our institute.

Journal of Experimental Biology (2016) 219, 508-515 doi:10.1242/jeb.127662

Preparation of FP-speract

Each FP-speract expression vector was transformed in the *E. coli* strain BL21(DE3). A single colony was grown in 50 ml LB medium with kanamycin (30 µg ml^{-1}) for 12 h at 37°C. Subsequently, 2 ml were transferred to 200 ml LB medium with kanamycin (30 µg ml^{-1}) and incubated at 37°C. When the OD_{600} reached 0.8, 300 µmol l^{-1} IPTG was added and the incubation continued at 30°C over 24 h. The cells were centrifuged (4000 ***g*** for 20 min at 4°C) and the pellet was washed three times with NaCl 150 mmol l^{-1}, Tris-HCl 10 mmol l^{-1}, pH 7.4 (solution A), and re-suspended with 8 ml of solution A containing cOmplete™. The cells were lysed by sonication with a GE50T Ultrasonic processor (three treatments of 30 s at 20 watts on ice separated by 1-min intervals) and centrifuged (15,000 ***g*** for 15 min at 4°C). The supernatant was passed through a nickel column, Ni-NTA Superflow and washed with solution A containing 50 mmol l^{-1} imidazole. Then, FP-speract was eluted with solution A containing 250 mmol l^{-1} imidazole. The purification process was carried out at room temperature. The concentration of each FP-speract was determined by the Bradford protein assay using bovine serum albumin (BSA) as a standard. For physiological measurements (V_m, pH_i and $[Ca^{2+}]_i$), we used 10 nmol l^{-1} of eCFP-speract that was determined by its absorbance (molar extinction coefficient of eCFP: 32,500 M^{-1} cm^{-1}). The quality of each purified FP-speract was confirmed by electrophoresis on a 15% SDS-PAGE (Fig. S1).

Fluorometric determinations

V_m, pH_i and $[Ca^{2+}]_i$ of *S. purpuratus* spermatozoa were determined using DiSC3(5), BCECF-AM and Fluo-4-AM, respectively, as previously reported (Beltrán et al., 2014). In the three cases, 10 nmol l^{-1} speract or 10 nmol l^{-1} eCFP-speract was added to stimulate the sperm, and the change in fluorescence was recorded over 1 min with an SLM8000 spectrofluorometer modified by Olis Global Works Software. V_m and pHi measurements were performed in DASW as well as in normal ASW. To normalize the $[Ca^{2+}]_i$ changes, the cells were permeabilized with 0.05% Triton X-100 and the maximum fluorescence of Fluo-4 was obtained in each recording.

Visualization of mVenus-speract binding to *L. pictus* sperm receptor

Lytechinus pictus sperm were diluted 10-fold in low-Ca^{2+} ASW and then 100-fold in ASW containing 0.1% BSA and 10 nmol l^{-1} mVenus-speract or 10 nmol l^{-1} mVenus-speract with 500 nmol l^{-1} speract (as competitor). The samples were centrifuged (1000 ***g*** for 7 min at 4°C) and the supernatant was discarded to remove the unbound protein. Sperm (25 µl suspensions) were attached to a three-well slide (Electron Microscopy Sciences) at 4°C for 1 h and fixed with 25 µl 4% paraformaldehyde in ASW for 10 min. Subsequently, the cells were washed three times with phosphate buffered saline (in mmol l^{-1}: 137 NaCl, 2.7 KCl, 10 Na_2HPO_4 and 1.8 KH_2PO_4, pH 7.4), and 5 µl of Citifluor were added to minimize fluorescence bleaching. The samples were protected with a coverslip (0.13–0.17 mm thick) and the edges were sealed with nail polish. The fluorescence of the mVenus-speract on the sperm was observed with a 100× objective on a Zeiss LSM510 confocal microscope using an argon laser (488 nm) for excitation. Sperm images were obtained with the LSM 5 Image Browser program.

Competitive binding assays with a chemically synthesized fluorescent speract analogue (F-speract)

Competitive binding assays using F-speract were performed as previously reported (Tatsu et al., 2002), with some modifications. In this work, we measured the fluorescence of 10 nmol l^{-1} of F-speract in *L. pictus* sperm suspension, which contained 10 nmol l^{-1} equivalents of the speract receptor, using a small-volume cuvette (45 µl). As a binding competitor, 1, 3.16, 10, 31.6, 100, 316 and 1000 nmol l^{-1} of either speract or mAmetrine-speract were added to the sample and their fluorescence intensities (λ_{ex} 494/λ_{em} 524 nm) were determined. Even though the fluorescence intensity of mAmetrine excited at 494 nm is quite small at the equivalent concentration of F-speract, its fluorescence at a much higher concentration is not negligible. Therefore, net F-speract fluorescence intensities were obtained by subtraction of the fluorescence intensities of mAmetrine-speract (in the sperm suspension) from the total fluorescence intensities.

FRET assays using eCFP-speract and mVenus-speract

A sperm suspension (*L. pictus*) containing 10 nmol l^{-1} equivalents of speract receptor was mixed with a combination of eCFP-speract and mVenus-speract in the presence or absence of 1 µmol l^{-1} speract. Two different compositions of ligands were used as follows; 5 nmol l^{-1} eCFP-speract and 5 nmol l^{-1} mVenus-speract for a 1/1 (donor/acceptor) ratio, and 2 nmol l^{-1} eCFP-speract and 8 nmol l^{-1} mVenus-speract for a 1/4 ratio. Subsequently, the emission spectrum (λ_{ex}=433 nm) of the sample (with and without competitor) was recorded in the spectrofluorometer.

Statistical analysis

Fluorescence spectra or intensities were acquired with 4.2 Olis Global Works Software and processed with Microsoft Excel or R project 3.0.1 (Freeware). In figures, all values represent the means± s.e.m. unless otherwise indicated. We performed at least three different experiments with three distinct sea urchins. The Shapiro–Wilk test showed that all data obtained in this study showed a normal distribution (P>0.05). Statistical significance was evaluated using the Student's *t*-test. Differences were considered statistically significant at P<0.05.

RESULTS

Design of FP-speract

It has been reported that modification of the amino terminus of speract by small molecules does not affect its ligand activity (Dangott and Garbers, 1984; Nishigaki and Darszon, 2000). Therefore, we decided to fuse speract with an FP at the amino terminus of this peptide ligand. Fig. 1 shows a schematic structure of FP-speract. Considering that a bulky FP could interfere with speract–receptor interactions, a relatively long spacer composed of seven non-structural amino acids (Gly-Gly-Gly-Ser-Gly-Gly-Gly) was inserted between the FP and speract. To facilitate the process of purification, we added 6xHis to the amino terminus of FP using a forward primer of PCR. As described in the Materials and methods, three different FP-speracts were produced in BL21(DE3) and purified by the Ni^{2+} column. The purified proteins have the expected molecular weights (~28 kDa) as indicated by a 15% SDS-PAGE (Fig. S1).

Speract and eCFP-speract induce similar V_m, pH_i and $[Ca^{2+}]_i$ changes in the sperm

To evaluate the activity of FP-speract, we first determined the capacity of eCFP-speract to induce physiological sperm responses: V_m changes and increases in pH_i and $[Ca^{2+}]_i$ using the fluorescent indicators $DiSC_3(5)$, BCECF-AM and Fluo-4-AM, respectively (Beltrán et al., 2014). Fluorescence signals of 10 nmol l^{-1} eCFP (λ_{ex}=433 nm, λ_{em}=476 nm) did not interfere with the fluorescence measurements of these indicators.

Journal of Experimental Biology

Journal of Experimental Biology (2016) 219, 508-515 doi:10.1242/jeb.127662

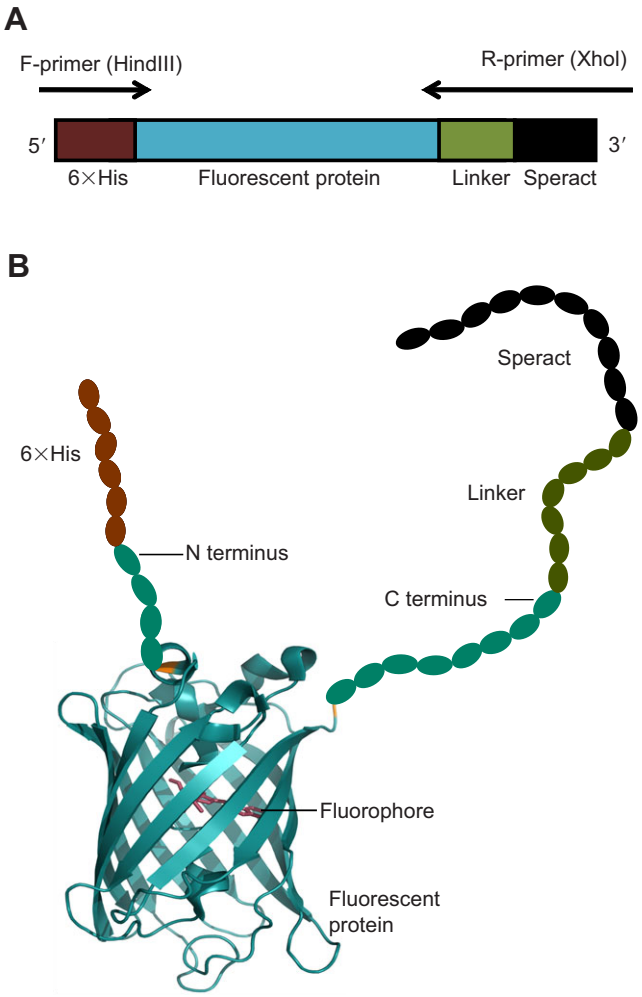

Fig. 1. Schematic structures of FP-speract. (A) An open reading frame of DNA that encodes an FP-speract (eCFP-speract). Forward primer (F-primer) encodes a HindIII site, 6×His and the N terminus of eCFP. Reverse primer (R-primer) encodes an XhoI site, speract, a flexible linker (GGGSGGG) and the C terminus of eCFP. (B) A structure of an FP-speract (eCFP-speract), in which a 3D structure of eCFP is shown in a ribbon diagram, along with 6×His residues at the N terminus of eCFP (brown ellipses) and the linker composed of the seven amino acids (dark green ellipses) followed by speract at the C terminus of eCFP (black ellipses). The ribbon diagram was prepared with the PyMOL trial version (Schrödinger). Some N- and C-terminal amino acids (MVSK and LGMDELYK, respectively) are not included in the crystal structure of eCFP (Lelimousin et al., 2009), so those amino acids were added as flexible terminal tails (cyan ellipses). mVenus-speract and mAmetrine-speract have basically the same structure.

Because the speract-induced initial hyperpolarization is difficult to detect in *S. purpuratus* sperm in normal ASW, we measured the V_m (as well as the pH_i) changes in swollen sperm in DASW, where the hyperpolarization can be easily observed (Babcock et al., 1992). Our results show that 10 nmol l^{-1} eCFP-speract and 10 nmol l^{-1} speract induce similar changes in V_m (Fig. 2A). Likewise, 10 nmol l^{-1} eCFP-speract elicited an increase in pH_i (Fig. 2B) and $[Ca^{2+}]_i$ (Fig. 2C), as intact speract does. It is worth mentioning that the magnitude of the pH_i increase induced by speract is larger in DASW than that observed in normal ASW (Fig. 2B). Considering that the sperm-specific Na^+/H^+ exchanger (sNHE) is activated by V_m hyperpolarization (Lee and Garbers, 1986) and that this hyperpolarization is larger in DASW (Fig. 2A), the enhanced increase in pH_i in DASW supports the involvement of sNHE in the signaling cascade of speract.

Visualization of mVenus-speract binding to the sperm receptor

We previously prepared F-speract as a synthetic fluorescent analogue of speract (Nishigaki and Darszon, 2000). F-speract is a useful speract analogue with which to study ligand–receptor interactions because its fluorescence quenches upon binding to its receptor. However, F-speract does not allow for the visualization of its binding to the receptor under fluorescence microscopy. In contrast, mVenus-speract maintained its fluorescence upon receptor binding and allowed us to visualize the localization of speract receptors with this fluorescent ligand (Fig. 3). In the presence of an excess of speract, the fluorescence signal of mVenus was not observed, indicating that the fluorescence signal from the sperm flagellum is specific.

Competitive binding activity of FP-speract using F-speract as a fluorescent probe

Although 10 nmol l^{-1} of both FP-speract and speract induced similar sperm responses (Fig. 2), it was necessary to perform quantitative experiments to precisely evaluate the activity of FP-speract. To this end, we performed a competitive binding assay using F-speract as a fluorescent probe, which is supposed to be the most efficient method to evaluate the ligand activity of speract analogues (Tatsu et al., 2002). For this experiment, we used *L. pictus* spermatozoa because the number of speract binding sites of this species is three times higher than that of *S. purpuratus*. One of the problems in performing this experiment is the fluorescence overlap between F-speract and FP-speract. As mentioned earlier, the fluorescence emission peak of eCFP is different from that of fluorescein (F-speract). However, a high concentration of eCFP completely masked the fluorescence signal of F-speract because of a significant fluorescence overlap between fluorescein and eCFP. Afterwards, we tried to use a blue FP (mEBFP2)-tagged speract for this experiment, but we were unable to produce a sufficient amount of the soluble mEBFP2-speract in BL21(DE3) for an unknown reason. We thus employed mAmetrine as a useful alternative for this purpose. mAmetrine is a yellow FP (λ_{em}=526 nm), with an excitation peak around 400 nm (Ai et al., 2008; Ding et al., 2011) that is classified as a large Stokes shift fluorophore (120 nm between excitation and emission peaks). Even though the fluorescence emission of mAmetrine excited by 490 nm is negligible compared with that obtained by excitation at 400 nm at a comparable concentration of F-speract, this small fluorescence intensity is not negligible at higher concentrations of the fluorophore. Therefore, for this experiment, we subtracted the fluorescence intensity of mAmetrine itself from the total fluorescence intensity to obtain the net F-speract quenching. Fig. 4 shows the competitive binding curves of mAmetrine-speract and speract upon F-speract binding to its receptor in *L. pictus* spermatozoa. The IC_{50} values of mAmetrine-speract and speract were 61±9 and 8±0.8 nmol l^{-1} (n=3), respectively, indicating that this fluorescent analogue of speract has 7.6-fold less affinity for the receptor than speract.

FRET measurements between eCFP-speract and mVenus-speract upon binding to the receptor

As mentioned in the Introduction, the speract receptor is a 77 kDa protein that possesses a single transmembrane segment. Although it has some sequence homology to the Cys-rich

Journal of Experimental Biology (2016) 219, 508-515 doi:10.1242/jeb.127662

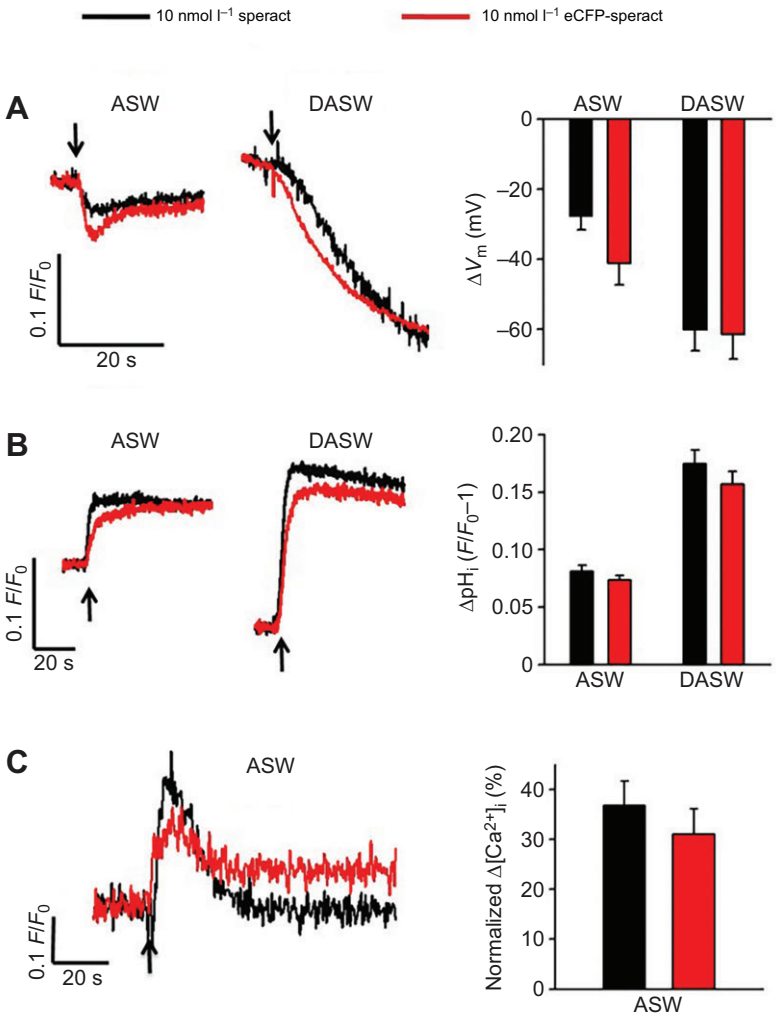

Fig. 2. Speract and eCFP-speract induce similar changes in membrane potential (V_m), intracellular pH (pH_i) and intracellular Ca^{2+} concentration ($[Ca^{2+}]_i$) in sperm. Left panels show representative *Strongylocentrotus purpuratus* sperm responses [(A) V_m, (B) pH_i and (C) $[Ca^{2+}]_i$)] to 10 nmol l^{-1} speract (black line) or 10 nmol l^{-1} eCFP-speract (red line). For V_m and pHi measurements, sperm responses were determined in diluted ASW (DASW) as well as in normal ASW. Arrows indicate ligand additions. F/F_0, change in fluorescence intensity relative to baseline. Right panels show averages of the maximum sperm responses to speract (black bars) or eCFP-speract (red bars), except for V_m hyperpolarization obtained in DASW at the end of the measurements. Error bars represent s.e.m. (n=3). There is no difference between the sperm responses induced by speract and those induced by eCFP-speract in any of the cases.

scavenger protein found in mammals, its biochemical properties have not been studied in detail (Dangott et al., 1989). To explore whether the speract receptors form an oligomer or exist as a monomer in sea urchin sperm, we performed a binding experiment based on FRET. Fig. 5 shows the fluorescence emission spectra (λ_{ex}=433 nm) of a mixture of 2 nmol l^{-1} eCFP-speract and 8 nmol l^{-1} mVenus-speract (1/4 ratio) with *L. pictus* spermatozoa (equivalent to 10 nmol l^{-1} speract receptor) in the presence or absence of an excess amount of speract. We observed a significant difference (15.1±2.0%, n=3) of CFP

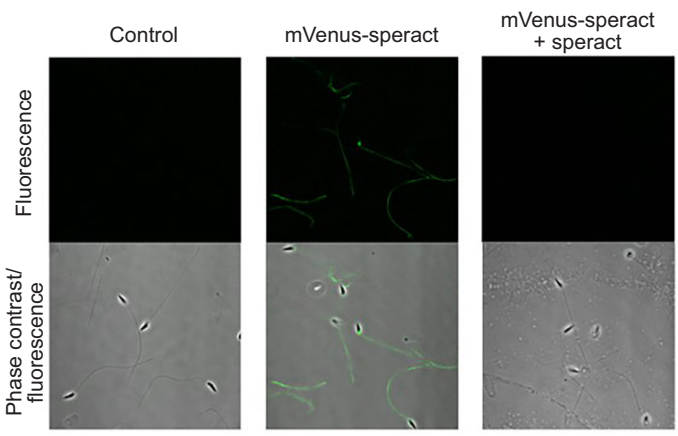

Fig. 3. mVenus-speract binds specifically to the flagellum. Upper panels show confocal fluorescence images and lower panels are the superposition of fluorescence and phase contrast images. The left panels are representative images obtained with *Lytechinus pictus* spermatozoa (control). Central panels show images of the spermatozoa treated with 10 nmol l^{-1} mVenus-speract. Right panels show images obtained in the presence of an excess of speract (500 nmol l^{-1}) with 10 nmol l^{-1} mVenus-speract.

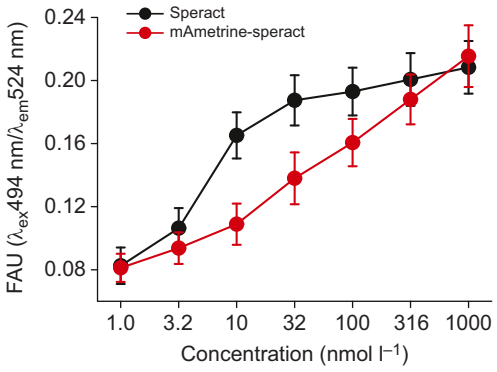

Fig. 4. mAmetrine-speract and speract have comparable affinities to the receptor in *Lytechinus pictus* spermatozoa. Recovery of fluorescence intensities of F-speract from the quenched state by the receptor competition using speract (black) and mAmetrine-speract (red) at different concentrations. Error bars represent ±s.e.m. (n=3). FAU, fluorescence arbitrary units.

Journal of Experimental Biology (2016) 219, 508-515 doi:10.1242/jeb.127662

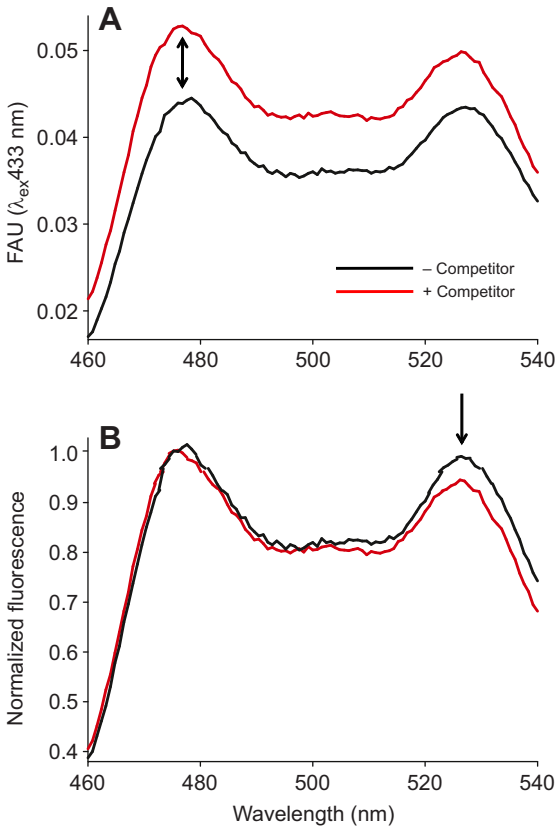

Fig. 5. A positive FRET signal is observed upon two-color (cyan and yellow) ligand binding to the speract receptor. (A) Representative fluorescence spectra of a mixture of 2 nmol l^{-1} eCFP-speract and 8 nmol l^{-1} mVenus-speract in *Lytechinus pictus* sperm suspension (equivalent to 10 nmol l^{-1} speract receptor) in the presence (red line) and absence (black line) of excess of speract (1 µmol l^{-1}) as competitor. FAU, fluorescence arbitrary units. A double-headed arrow indicates the peak fluorescence of eCFP. (B) Normalized fluorescence spectra of the two conditions. The two spectra are not identical because of the occurrence of FRET; fluorescence spectra around 528 nm (the peak of mVenus fluorescence, indicated by arrow) without the competitor is slightly higher than that in the presence of the competitor.

fluorescence intensities between the two conditions (Fig. 5A). In the normalized fluorescence spectra (Fig. 5B), the fluorescence intensities around 528 nm, which correspond to the fluorescence peak of mVenus (Nagai et al., 2002), are higher in the absence of the competitor than those in the presence. These results indicate that there is FRET between these two speract analogues when they are bound to the receptor, suggesting that the speract receptors exist as a cluster forming an oligomer, at least a dimer, on the sperm plasma membrane. Alternatively, a single speract receptor protein possesses multiple binding sites for this ligand.

DISCUSSION

Development of FP-speract

In this study, we prepared a recombinant speract analogue tagged with an FP (FP-speract, Fig. 1) and evaluated its functionality. In spite of the relatively large size of FP (25 kDa) compared with speract (decapeptide), FP-speract induced physiological sperm responses (V_m, pH_i and $[Ca^{2+}]_i$) in a manner similar to that of speract (Fig. 2). The competitive binding curves of FP-speract and speract (Fig. 4) indicate that FP-speract maintained a comparable affinity to the receptor (only 7.6-fold less potent than intact speract), confirming that FP-speract is indeed a useful ligand for spermatozoa. A non-structural seven-amino-acid spacer between FP and speract probably facilitated this favorable result. To our knowledge, there are a few cases of functional FP-tagged peptide ligands such as parathyroid hormone and bradykinin (Charest-Morin et al., 2013). Although both are functional ligands and induce the expected cell responses, the exact affinity to the corresponding receptor has not been determined.

Application of FP-speract to determine the formation of clusters by the speract receptor

Previously, we prepared fluorescent speract analogues tagged with fluorescein (F-speract), whose fluorescence quenches upon binding to its receptor (Nishigaki and Darszon, 2000). In contrast, FP-speract maintains its fluorescence even after binding to its receptor (Fig. 3). Taking advantage of this property, we applied two color variants of FP-speract, cyan and yellow, to study the proximity of the speract binding sites.

The receptors for resact and asterosap are known to be membrane-bound GC (Matsumoto et al., 2003; Singh et al., 1988). Previously, it was estimated that there are approximately 100,000 asterosap binding sites in the starfish sperm flagellum (Nishigaki et al., 2000). Recently, it was reported that a single cell of *A. punctulata* spermatozoa possesses 300,000 molecules of GC (Pichlo et al., 2014). Comparing these numbers, the speract receptors are less abundant: 60,000 binding sites in *L. pictus* and 20,000 binding sites in *S. purpuratus* (Nishigaki et al., 2001). The speract receptor is a 77 kDa Cys-rich protein distinct from GC that is supposed to be coupled to GC (Dangott and Garbers, 1984; Dangott et al., 1989). It is known that the receptor for the atrial natriuretic peptide, a membrane-bound guanylyl cyclase A, exists as a dimer (Chinkers and Wilson, 1992; Ogawa et al., 2004). However, there is no such information for SAP receptors either in resact-type receptors (GC) or in speract-type receptors.

In this study, we explored the proximity between the speract binding sites on the sperm plasma membrane using multicolor FP-speract. Conventional optical microscopy is unable to resolve the distance between two objects localized at less than 200 nm. In contrast, the current techniques of super-resolution microscopy can increase the resolution up to 20 nm (Fernández-Suárez and Ting, 2008; Huang et al., 2009). However, those techniques require sophisticated experimental conditions and analyses. Therefore, we performed a FRET measurement using cyan and yellow variants of FP-speract. In practice, we can obtain higher spatial resolution applying FRET (<10 nm) than with super-resolution microscopy (Fernández-Suárez and Ting, 2008; Huang et al., 2009). It was reported that the Förster distance (50% of FRET) between eCFP and mVenus is estimated to be around 5 nm (Patterson et al., 2000). Because FRET efficiency decreases by a function of the sixth power of the distance, twice the Förster distance (10 nm in this study) should result in less than 2% FRET efficiency. In this work, we obtained approximately 15% FRET efficiency in our experimental condition (1/4 donor/acceptor ratio). When we performed the same experiment using the 1/1 ratio, the FRET efficiency was lower (10.1±0.8%, n=4), probably because larger fractions of the adjacent binding sites were occupied with the donor fluorophore in this condition. Although the speract receptors are abundant in the plasma membrane of *L. pictus* sperm flagella (60,000 binding sites per cell), the average distance between the binding sites is estimated to be approximately 40 nm if the binding sites are homogeneously distributed on the plasma membrane of the sperm flagellum (0.3 µm diameter and 45 µm long). Therefore, our results (Fig. 5) suggest

that the speract binding sites are not homogeneously distributed, but exist as clusters. This is the first experimental evidence about a cluster formation of SAP receptors. Considering that the speract receptor contains four repeats of Cys-rich domains (Dangott et al., 1989), we cannot rule out the possibility that the single polypeptide receptor has multiple speract binding sites. Further experiments, such as precise determination of molecular stoichiometry between speract receptor and speract binding sites, are required to address this question. It was reported that the speract receptor is localized in a lipid raft (Loza-Huerta et al., 2013; Ohta et al., 2000), which may partially explain its formation of the clusters. Regardless of the type of cluster (intermolecular, intramolecular or both), a cluster of binding sites might provide cooperative bindings, as reported in speract and other SAPs (Nishigaki et al., 2000, 2001; Pichlo et al., 2014).

FP-speract as a tool for experimental training

The sea urchin has been used as a classical and excellent model to observe the process of fertilization in the field of reproductive and developmental biology. Although it is not trivial to document sperm chemotaxis in some species, it is quite easy to observe speract (SAPs in general) activity by recovering suppressed sperm motility in slightly acidified seawater (see Movie 1) (Ohtake, 1976). Considering that preparation of recombinant protein expressed in *E. coli* is a standard protocol in molecular biology, FP-speract would be quite useful for experimental training. The coloration of a FP-speract facilitates the visualization of the modified speract throughout the preparation along with the determination of its protein concentration.

Conclusions

In this study, we developed recombinant speract analogs tagged with an FP (FP-speract). Although the size of the fluorescent tag is more than 20 times larger than this ligand, FP-speract maintains activity comparable to that of speract, indicating that FP-speract is a useful tool with which to study the action of this peptide on spermatozoa. Using cyan and yellow variants of FP-speract, we were able to determine a cluster formation of the speract binding sites, which might imply some roles for positive and/or negative cooperativity in speract–receptor interactions. We believe that FP-speract is a useful tool not only for scientific research but also for experimental training. Furthermore, FP-tagged recombinant peptide could be generally useful for other types of peptide ligand.

Acknowledgements

We thank Dr T. Nagai (Osaka University), Dr A. Miyawaki (RIKEN) and Dr R. Campbell (University of Alberta) for providing eCFP-pRSETB, mVenus-pRSETB and pmAmetrine1.2, respectively, and Dr Y. Tatsu (AIST, Ikeda) for providing synthetic speract. We are grateful to the National Institute of Genetics (Mishima, Japan) for providing two *E. coli* strains, JM109(DE3) and BL21(DE3). We thank T. Olamendi (IBT-UNAM) for HPLC analysis of F-speract, X. Alvarado (IBT-UNAM) for the confocal images, and E. López, S. Becerra, J Yañez and P. Gaytán (IBT-UNAM) for oligonucleotide synthesis and DNA sequencing of plasmids. We thank A. Blancas (IBT-UNAM) for taking care of the sea urchins. We appreciate Dr A. Darszon's critical reading of the manuscript. We thank T. Liévano for reviewing the English grammar of the manuscript. We also thank an anonymous reviewer for their suggestion to improve our FRET experiment.

Competing interests

The authors declare no competing or financial interests.

Author contributions

C.A.-H. performed almost all experiments and prepared all figures, F.R. prepared the plasmid encoding eCFP-speract, Y.S.-G. supervised preparation of plasmids encoding mVenus-speract and mAmetrine-speract and all recombinant proteins, C.B. supervised determination of all sperm physiological responses and visualization of speract binding site, and T.N. designed the entire project and wrote the manuscript. All authors participated in the interpretation of results and reviewed the manuscript.

Funding

This work was supported by Dirección General de Asuntos del Personal Académico - Programa de Apoyo a Proyectos de Investigación e Innovación Tecnológica (DGAPA-PAPIIT) - UNAM [IN204112 to C.B. and IN203513 to T.N.] and by Consejo Nacional de Ciencia y Tecnología (CONACyT) [128566 and 177138 to T.N.]. F.R. and Y.S.-G. are PhD students supported by CONACyT.

Supplementary information

Supplementary information available online at http://jeb.biologists.org/lookup/suppl/doi:10.1242/jeb.127662/-/DC1

References

Ai, H.-W., Hazelwood, K. L., Davidson, M. W. and Campbell, R. E. (2008). Fluorescent protein FRET pairs for ratiometric imaging of dual biosensors. *Nat. Methods* **5**, 401-403.

Alvarez, L., Dai, L., Friedrich, B. M., Kashikar, N. D., Gregor, I., Pascal, R. and Kaupp, U. B. (2012). The rate of change in Ca^{2+} concentration controls sperm chemotaxis. *J. Cell Biol.* **196**, 653-663.

Babcock, D. F., Bosma, M. M., Battaglia, D. E. and Darszon, A. (1992). Early persistent activation of sperm K^+ channels by the egg peptide speract. *Proc. Natl. Acad. Sci. USA* **89**, 6001-6005.

Beltrán, C., Rodríguez-Miranda, E., Granados-González, G., García de De la Torre, L., Nishigaki, T. and Darszon, A. (2014). Zn^{2+} induces hyperpolarization by activation of a K^+ channel and increases intracellular Ca^{2+} and pH in sea urchin spermatozoa. *Dev. Biol.* **394**, 15-23.

Böhmer, M., Van, Q., Weyand, I., Hagen, V., Beyermann, M., Matsumoto, M., Hoshi, M., Hildebrand, E. and Kaupp, U. B. (2005). Ca^{2+} spikes in the flagellum control chemotactic behavior of sperm. *EMBO J.* **24**, 2741-2752.

Charest-Morin, X., Fortin, J.-P., Bawolak, M.-T., Lodge, R. and Marceau, F. (2013). Green fluorescent protein fused to peptide agonists of two dissimilar G protein-coupled receptors: novel ligands of the bradykinin B2 (rhodopsin family) receptor and parathyroid hormone PTH1 (secretin family) receptor. *Pharmacol. Res. Perspect.* **1**, e00004.

Chinkers, M. and Wilson, E. M. (1992). Ligand-independent oligomerization of natriuretic peptide receptors. Identification of heteromeric receptors and a dominant negative mutant. *J. Biol. Chem.* **267**, 18589-18597.

Dangott, L. J. and Garbers, D. L. (1984). Identification and partial characterization of the receptor for speract. *J. Biol. Chem.* **259**, 13712-13716.

Dangott, L. J., Jordan, J. E., Bellet, R. A. and Garbers, D. L. (1989). Cloning of the mRNA for the protein that crosslinks to the egg peptide speract. *Proc. Natl. Acad. Sci. USA* **86**, 2128-2132.

Darszon, A., Nishigaki, T., Beltran, C. and Trevino, C. L. (2011). Calcium channels in the development, maturation, and function of spermatozoa. *Physiol. Rev.* **91**, 1305-1355.

Ding, Y., Ai, H.-W., Hoi, H. and Campbell, R. E. (2011). Förster resonance energy transfer-based biosensors for multiparameter ratiometric imaging of Ca^{2+} dynamics and caspase-3 activity in single cells. *Anal. Chem.* **83**, 9687-9693.

Ducancel, F., Matre, V., Dupont, C., Lajeunesse, E., Wollberg, Z., Bdolah, A., Kochva, E., Boulain, J. C. and Menez, A. (1993). Cloning and sequence analysis of cDNAs encoding precursors of sarafotoxins. Evidence for an unusual "rosary-type" organization. *J. Biol. Chem.* **268**, 3052-3055.

Fernández-Suárez, M. and Ting, A. Y. (2008). Fluorescent probes for super-resolution imaging in living cells. *Nat. Rev. Mol. Cell Biol.* **9**, 929-943.

Galindo, B. E., Beltrán, C., Cragoe, E. J., Jr. and Darszon, A. (2000). Participation of a K^+ channel modulated directly by cGMP in the speract-induced signaling cascade of *Strongylocentrotus purpuratus* sea urchin sperm. *Dev. Biol.* **221**, 285-294.

Garbers, D. L. (1989). Molecular basis of fertilization. *Annu. Rev. Biochem.* **58**, 719-742.

Garbers, D. L., Watkins, H. D., Hansbrough, J. R., Smith, A. and Misono, K. S. (1982). The amino acid sequence and chemical synthesis of speract and of speract analogues. *J. Biol. Chem.* **257**, 2734-2737.

Guerrero, A., Nishigaki, T., Carneiro, J., Yoshiro Tatsu, J., Wood, C. D. and Darszon, A. (2010). Tuning sperm chemotaxis by calcium burst timing. *Dev. Biol.* **344**, 52-65.

Huang, B., Bates, M. and Zhuang, X. (2009). Super-resolution fluorescence microscopy. *Annu. Rev. Biochem.* **78**, 993-1016.

Kaupp, U. B., Solzin, J., Hildebrand, E., Brown, J. E., Helbig, A., Hagen, V., Beyermann, M., Pampaloni, F. and Weyand, I. (2003). The signal flow and motor response controlling chemotaxis of sea urchin sperm. *Nat. Cell Biol.* **5**, 109-117.

Kaupp, U. B., Kashikar, N. D. and Weyand, I. (2008). Mechanisms of sperm chemotaxis. *Annu. Rev. Physiol.* **70**, 93-117.

Kinoh, H., Shimizu, T., Fujimoto, H. and Suzuki, N. (1994). Expression of a putative precursor mRNA for sperm-activating peptide I in accessory cells of the

ovary in the sea urchin *Hemicentrotus pulcherrimus*. *Roux's Arch. Dev. Biol.* **203**, 381-388.

Kotera, I., Iwasaki, T., Imamura, H., Noji, H. and Nagai, T. (2010). Reversible dimerization of *Aequorea victoria* fluorescent proteins increases the dynamic range of FRET-based indicators. *ACS Chem. Biol.* **5**, 215-222.

Lee, H. C. and Garbers, D. L. (1986). Modulation of the voltage-sensitive Na^+/H^+ exchange in sea urchin spermatozoa through membrane potential changes induced by the egg peptide speract. *J. Biol. Chem.* **261**, 16026-16032.

Lelimousin, M., Noirclerc-Savoye, M., Lazareno-Saez, C., Paetzold, B., Le Vot, S., Chazal, R., Macheboeuf, P., Field, M. J., Bourgeois, D. and Royant, A. (2009). Intrinsic dynamics in ECFP and Cerulean control fluorescence quantum yield. *Biochemistry* **48**, 10038-10046.

Loza-Huerta, A., Vera-Estrella, R., Darszon, A. and Beltrán, C. (2013). Certain *Strongylocentrotus purpuratus* sperm mitochondrial proteins co-purify with low density detergent-insoluble membranes and are PKA or PKC-substrates possibly involved in sperm motility regulation. *Biochim. Biophys. Acta* **1830**, 5305-5315.

Matsumoto, M., Briones, A. V., Nishigaki, T. and Hoshi, M. (1999). Sequence analysis of cDNAs encoding precursors of starfish asterosaps. *Dev. Genet.* **25**, 130-136.

Matsumoto, M., Solzin, J., Helbig, A., Hagen, V., Ueno, S., Kawase, O., Maruyama, Y., Ogiso, M., Godde, M., Minakata, H. et al. (2003). A sperm-activating peptide controls a cGMP-signaling pathway in starfish sperm. *Dev. Biol.* **260**, 314-324.

Nagai, T., Ibata, K., Park, E. S., Kubota, M., Mikoshiba, K. and Miyawaki, A. (2002). A variant of yellow fluorescent protein with fast and efficient maturation for cell-biological applications. *Nat. Biotechnol.* **20**, 87-90.

Nakachi, M., Hoshi, M., Matsumoto, M. and Moriyama, H. (2008). Conserved sequences of sperm-activating peptide and its receptor throughout evolution, despite speciation in the sea star *Asterias amurensis* and closely related species. *Zygote* **16**, 229-237.

Nishigaki, T. and Darszon, A. (2000). Real-time measurements of the interactions between fluorescent speract and its sperm receptor. *Dev. Biol.* **223**, 17-26.

Nishigaki, T., Chiba, K., Miki, W. and Hoshi, M. (1996). Structure and function of asterosaps, sperm-activating peptides from the jelly coat of starfish eggs. *Zygote* **4**, 237-245.

Nishigaki, T., Chiba, K. and Hoshi, M. (2000). A 130-kDa membrane protein of sperm flagella is the receptor for asterosaps, sperm-activating peptides of starfish *Asterias amurensis*. *Dev. Biol.* **219**, 154-162.

Nishigaki, T., Zamudio, F. Z., Possani, L. D. and Darszon, A. (2001). Time-resolved sperm responses to an egg peptide measured by stopped-flow fluorometry. *Biochem. Biophys. Res. Commun.* **284**, 531-535.

Nomura, K. and Isaka, S. (1985). Synthetic study on the structure-activity relationship of sperm activating peptides from the jelly coat of sea urchin eggs. *Biochem. Biophys. Res. Commun.* **126**, 974-982.

Ogawa, H., Qiu, Y., Ogata, C. M. and Misono, K. S. (2004). Crystal structure of hormone-bound atrial natriuretic peptide receptor extracellular domain: rotation mechanism for transmembrane signal transduction. *J. Biol. Chem.* **279**, 28625-28631.

Ohta, K., Sato, C., Matsuda, T., Toriyama, M., Vacquier, V. D., Lennarz, W. J. and Kitajima, K. (2000). Co-localization of receptor and transducer proteins in the glycosphingolipid-enriched, low density, detergent-insoluble membrane fraction of sea urchin sperm. *Glycoconj. J.* **17**, 205-214.

Ohtake, H. (1976). Respiratory behaviour of sea-urchin spermatozoa. I. Effect of pH and egg water on the respiratory rate. *J. Exp. Zool.* **198**, 303-311.

Patterson, G. H., Piston, D. W. and Barisas, B. G. (2000). Förster distances between green fluorescent protein pairs. *Anal. Biochem.* **284**, 438-440.

Pichlo, M., Bungert-Plumke, S., Weyand, I., Seifert, R., Bonigk, W., Strunker, T., Kashikar, N. D., Goodwin, N., Muller, A., Korschen, H. G. et al. (2014). High density and ligand affinity confer ultrasensitive signal detection by a guanylyl cyclase chemoreceptor. *J. Cell Biol.* **206**, 541-557.

Podolsky, R. D. (2002). Fertilization ecology of egg coats: physical versus chemical contributions to fertilization success of free-spawned eggs. *J. Exp. Biol.* **205**, 1657-1668.

Ramarao, C. S., Burks, D. J. and Garbers, D. L. (1990). A single mRNA encodes multiple copies of the egg peptide speract. *Biochemistry* **29**, 3383-3388.

Reynaud, E., De de La Torre, L., Zapata, O., Lievano, A. and Darszon, A. (1993). Ionic bases of the membrane potential and intracellular pH changes induced by speract in swollen sea urchin sperm. *FEBS Lett.* **329**, 210-214.

Seifert, R., Flick, M., Bonigk, W., Alvarez, L., Trotschel, C., Poetsch, A., Muller, A., Goodwin, N., Pelzer, P., Kashikar, N. D. et al. (2015). The CatSper channel controls chemosensation in sea urchin sperm. *EMBO J.* **34**, 379-392.

Singh, S., Lowe, D. G., Thorpe, D. S., Rodriguez, H., Kuang, W.-J., Dangott, L. J., Chinkers, M., Goeddel, D. V. and Garbers, D. L. (1988). Membrane guanylate cyclase is a cell-surface receptor with homology to protein kinases. *Nature* **334**, 708-712.

Strünker, T., Weyand, I., Bönigk, W., Van, Q., Loogen, A., Brown, J. E., Kashikar, N., Hagen, V., Krause, E. and Kaupp, U. B. (2006). A K^+-selective cGMP-gated ion channel controls chemosensation of sperm. *Nat. Cell Biol.* **8**, 1149-1154.

Suzuki, N. (1995). Structure, function and biosynthesis of sperm-activating peptides and fucose sulfate glycoconjugate in the extracellular coat of sea urchin eggs. *Zoolog. Sci.* **12**, 13-27.

Tatsu, Y., Nishigaki, T., Darszon, A. and Yumoto, N. (2002). A caged sperm-activating peptide that has a photocleavable protecting group on the backbone amide. *FEBS Lett.* **525**, 20-24.

Wood, C. D., Nishigaki, T., Furuta, T., Baba, S. A. and Darszon, A. (2005). Real-time analysis of the role of Ca^{2+} in flagellar movement and motility in single sea urchin sperm. *J. Cell Biol.* **169**, 725-731.